Efficient Extension to Quadrilateral Element of Three Field Hu-Washizu 2D Elasticity Formulation Based on Biorthogonal Systems

B.P. Lamichhane[1], M.Pingaro[2,*], P.Venini[2,*]

Abstract

New quadrilateral mixed finite element based on modified Hu-Washizu formulation are presented. Hu-Washizu is a three field formulation where the unknowns are: displacement, stress and strain. The stability and consistency of the element are obtained by adding differnt types of bubble functions at the displacement field. Different types of bubble functions are successfully investigated and analyzed. In order to obtain an efficient discretization scheme, we use a pair of finite element bases forming a biorthogonal system for the strain and stress. The biorthogonality relation allows us to statically condense out the strain and stress from the saddle-point system leading to a symmetric and positive-definite system. The strain and stress can be recovered in a post-processing step simply by inverting a diagonal matrix. Numerical examples prove the efficiency and the stability of the elements in the case of incompressible limit and distorted meshes. The extension at the 3D case is straightforward.

Keywords: mixed finite elements, quadrilateral element, Hu-Washizu, biorthogonal systems, elasticity.

*Corresponding author.

Email addresses: Bishnu.Lamichhane@newcastle.edu.au (B.P. Lamichhane), marco.pingaro@iusspavia.it (M.Pingaro), paolo.venini@unipv.it (P.Venini)

[1]School of Mathematical and Physical Sciences, University of Newcastle, Callaghan, NSW 2308

[2]Department of Civil Engineering and Architecture, University of Pavia, Pavia, Italy

1. Introduction

In the linear and non-linear elasticity when the Lamé constant λ tends to infinity the standard finite element exhibit some problem of convergence may be locking phenomena. In this context mixed formulations are used to solve this inconvenient. One of the most popular mixed formulation adopted is the Hellinger-Raisner formulation, in that we describe the problem using with variables the stresses and the displacements. This type of formulation requires the fulfillment of the inf-sup condition as described in D.Boffi et al. (2013). For the Hellinger-Reissner formulation many elements are created such as D.N.Arnold and R.Winther (2002) for triangle elements and D.N.Arnold and G.Awanou (2005) for quadrilateral. Another type of formulation is the Hu-Washizu formulation (see H.Hu (1955); K.Washizu (1982)) that it was a three-field formulation. This was first introduced by B.M.Fraeijs de Veubeke (1951). One examples of Hu-Washizu formulation applied at linear and non-linear elasticity using quadrilaterals and hexahedra are reported in E.P. Kasper and R.L. Taylor (2000,?). In B.P.Lamichhane et al. (2006) are showed that the modify Hu-Washizu formulation are able to obtaining uniform convergence of the finite nelement approximation in the nearly incompressible regime in the case of quadrilateral elements. The goal of this work is to present an extension using the quadrilateral elements of the modified three-field formulation Hu-Washizu presented in B.P.Lamichhane (2009). In accordance to B.P.Lamichhane et al. (2013) we adopt the idea to create a biorthogonal system between the stresses and strains. This assumption is essentially for the static condensation of the stresses and strains for obtain a linear system in the only unknown displacement field. In order to ensure the stability of the element we enrich the space of displacement field with different type of bubble functions in accordance to W.Bai (1997); B.P.Lamichhane (2015) for the Stokes problem. In W.Bai (1997) we adopt two bubble functions to stabilize the element, while in B.P.Lamichhane (2015) use one single bubble function.

The structure of the papers are the following: first of all in Section 2 we recall the basic equations of linear elastic problem, in Section 3 we briefly recall the modified Hu-Washizu formulations, Section 4 we develop the finite element spaces. Finally in Section 5 we report some examples using the studied element and in Section 6 the conclusions of the work are detailed.

2. Linear elastic continuum problem

In this section we briefly recovery the equations governing the linear elastic problem. The equilibrium equation is:

$$-\mathrm{div}(\boldsymbol{\sigma}) = \boldsymbol{f}\,, \tag{1}$$

while in small deformation is:

$$\boldsymbol{d} = \boldsymbol{\varepsilon}(\boldsymbol{u}) = \frac{1}{2}(\boldsymbol{\nabla}\,\boldsymbol{u} + \boldsymbol{\nabla}\,\boldsymbol{u}^T)\,. \tag{2}$$

In the case of linear elasticity we have:

$$\boldsymbol{\sigma} = \lambda\, tr(\boldsymbol{\varepsilon})\boldsymbol{I} + 2\mu\,\boldsymbol{\varepsilon} \tag{3}$$

where μ and λ are the Lamé constant. By some algebra one obtains:

$$\boldsymbol{\sigma} = \begin{pmatrix} \lambda(\varepsilon_{11}+\varepsilon_{22}) & 0 \\ 0 & \lambda(\varepsilon_{11}+\varepsilon_{22}) \end{pmatrix} + 2\mu \begin{pmatrix} \varepsilon_{11} & \varepsilon_{12} \\ \varepsilon_{12} & \varepsilon_{22} \end{pmatrix}\,, \tag{4}$$

and rearranging the equation (4):

$$\boldsymbol{\sigma} = \begin{pmatrix} (\lambda+2\mu)\varepsilon_{11} + \lambda\,\varepsilon_{22} & 2\mu\,\varepsilon_{12} \\ 2\mu\,\varepsilon_{12} & (\lambda+2\mu)\,\varepsilon_{22} + \lambda\,\varepsilon_{11} \end{pmatrix}\,. \tag{5}$$

3. Briefly introduction to modify Hu-Washizu

We define the trial variables: $\boldsymbol{\varepsilon}(\boldsymbol{u})$, $\boldsymbol{d}$ and $\boldsymbol{\sigma}$, while the test variables are: $\boldsymbol{\varepsilon}(\boldsymbol{v})$, $\boldsymbol{e}$ and $\boldsymbol{\tau}$.

$$-\int_\Omega \mathrm{div}(\boldsymbol{C} : \boldsymbol{d})) \cdot \boldsymbol{v} = \boldsymbol{f} \tag{6}$$

$$\begin{aligned} a((\boldsymbol{u},\boldsymbol{d}),(\boldsymbol{v},\boldsymbol{e})) + b((\boldsymbol{v},\boldsymbol{e}),\boldsymbol{\sigma}) &= l(\boldsymbol{v}) && (7)\\ b((\boldsymbol{u},\boldsymbol{d}),\boldsymbol{\tau}) &= 0 && (8) \end{aligned}$$

where:

$$\begin{aligned} a((\boldsymbol{u},\boldsymbol{d}),(\boldsymbol{v},\boldsymbol{e})) &= \int_\Omega \boldsymbol{d} : (\boldsymbol{C} : \boldsymbol{e})\, dx + \alpha \int_\Omega (\boldsymbol{\varepsilon}(\boldsymbol{u}) - \boldsymbol{d}) : (\boldsymbol{\varepsilon}(\boldsymbol{v}) - \boldsymbol{e})\, dx && (9)\\ b((\boldsymbol{u},\boldsymbol{d}),\boldsymbol{\tau}) &= \int_\Omega (\boldsymbol{\varepsilon}(\boldsymbol{u}) - \boldsymbol{d}) : \boldsymbol{\tau}\, dx\,. && (10) \end{aligned}$$

The modify weak formulation of the problem is:

$$\begin{cases} \alpha \int_\Omega (\boldsymbol{\varepsilon}(\boldsymbol{u}) - \boldsymbol{d}) : \boldsymbol{\varepsilon}(\boldsymbol{v})\, dx + \int_\Omega \boldsymbol{\varepsilon}(\boldsymbol{v}) : \boldsymbol{\sigma}\, dx = \int_\Omega \boldsymbol{f} \cdot \boldsymbol{v}\, dx \\ \int_\Omega \boldsymbol{d} : \boldsymbol{C}\boldsymbol{e}\, dx - \alpha \int_\Omega (\boldsymbol{\varepsilon}(\boldsymbol{u}) - \boldsymbol{d}) : \boldsymbol{e}\, dx - \int_\Omega \boldsymbol{e} : \boldsymbol{\sigma}\, dx = 0 \\ \int_\Omega (\boldsymbol{\varepsilon}(\boldsymbol{u}) - \boldsymbol{d}) : \boldsymbol{\tau}\, dx = 0 \end{cases} \tag{11}$$

by rearranging:

$$\begin{cases} \alpha \int_\Omega \boldsymbol{\varepsilon}(\boldsymbol{u}) : \boldsymbol{\varepsilon}(\boldsymbol{v})\, dx - \alpha \int_\Omega \boldsymbol{d} : \boldsymbol{\varepsilon}(\boldsymbol{v})\, dx + \int_\Omega \boldsymbol{\varepsilon}(\boldsymbol{v}) : \boldsymbol{\sigma}\, dx & = \int_\Omega \boldsymbol{f} \cdot \boldsymbol{v}\, dx \\ -\alpha \int_\Omega \boldsymbol{\varepsilon}(\boldsymbol{u}) : \boldsymbol{e}\, dx + \int_\Omega \boldsymbol{d} : \boldsymbol{C}\boldsymbol{e}\, dx + \alpha \int_\Omega \boldsymbol{d} : \boldsymbol{e}\, dx - \int_\Omega \boldsymbol{e} : \boldsymbol{\sigma}\, dx & = 0 \\ \int_\Omega \boldsymbol{\varepsilon}(\boldsymbol{u}) : \boldsymbol{\tau}\, dx - \int_\Omega \boldsymbol{d} : \boldsymbol{\tau}\, dx & = 0 \end{cases} \tag{12}$$

It is possible to rewrite the system in equation (12) in matrix form in the following way:

$$\begin{bmatrix} \alpha \boldsymbol{A} & -\alpha \boldsymbol{B} & \boldsymbol{W} \\ -\alpha \boldsymbol{B}^T & \boldsymbol{K} + \alpha \boldsymbol{M} & -\boldsymbol{D} \\ \boldsymbol{W}^T & -\boldsymbol{D}^T & \boldsymbol{0} \end{bmatrix} \begin{bmatrix} \boldsymbol{x}_u \\ \boldsymbol{x}_d \\ \boldsymbol{x}_\sigma \end{bmatrix} = \begin{bmatrix} \boldsymbol{b}_f \\ \boldsymbol{0} \\ \boldsymbol{0} \end{bmatrix}, \tag{13}$$

where $\boldsymbol{A} = \int_\Omega \boldsymbol{\varepsilon}(\boldsymbol{u}) : \boldsymbol{\varepsilon}(\boldsymbol{v})$, $\boldsymbol{B} = \int_\Omega \boldsymbol{d} : \boldsymbol{\varepsilon}(\boldsymbol{v})$, $\boldsymbol{W} = \int_\Omega \boldsymbol{\sigma} : \boldsymbol{\varepsilon}(\boldsymbol{v})$, $\boldsymbol{K} = \int_\Omega \boldsymbol{C}\boldsymbol{e} : \boldsymbol{d}$, $\boldsymbol{M} = \int_\Omega \boldsymbol{e} : \boldsymbol{d}$, $\boldsymbol{D} = \int_\Omega \boldsymbol{\sigma} : \boldsymbol{e}$. $\boldsymbol{D}$ is a diagonal matrix. Using this property it is possible condense statically $\boldsymbol{x}_d$ and $\boldsymbol{x}_\sigma$, and we obtain the following system in the only unknown $\boldsymbol{x}_u$:

$$\left[\alpha \boldsymbol{A} - \alpha \left(\boldsymbol{B}\boldsymbol{D}^{-1}\boldsymbol{W}^{-T} + \boldsymbol{W}\boldsymbol{D}^{-1}\boldsymbol{B}^T\right) + \boldsymbol{W}\boldsymbol{D}^{-1}\left(\boldsymbol{K} + \alpha \boldsymbol{M}\right)\boldsymbol{D}^{-1}\boldsymbol{W}^T\right] \boldsymbol{x}_u = \boldsymbol{b}_f \tag{14}$$

4. Finite element discretization

We consider a quasi-uniform triangulation $\mathcal{T}_h$ of the polygonal domain Ω consists of simply, either quadrilateral or hexahedral. We take into account of standard bilinear finite element space $K_h \subset H^1(\Omega)$ defined on the triangulation $\mathcal{T}_h$, where:

$$K_h := \left\{ v \in C^0(\Omega) : v_{|T} \in \mathcal{Q}_1(T),\, T \in \mathcal{T}_h \right\}, \quad K_h^0 = K_h \cap H_0^1(\Omega), \tag{15}$$

and the space of bubble functions

$$B_h := \left\{ b_T \in H^1(T) : b_{T|\partial T} = 0 \text{ and } \int_T b_T \, dx > 0,\ T \in \mathcal{T}_h \right\}, \tag{16}$$

and we define the spaces for strain and displacement as $\boldsymbol{S}_h := [K_h]^{2\times 2}$ and $\boldsymbol{V}_h := [K_h^0 \bigoplus B_h]^2$. In the next section we discuss the different choosing of bubble functions. For the discrete stress space we use:

$$\boldsymbol{M}_h := \left\{ \boldsymbol{\tau}_h \in [M_h]^{2\times 2} : \int_\Omega \boldsymbol{\tau}_h : \mathbf{1} \, dx = 0 \right\} \subset \boldsymbol{S}_0 \,, \tag{17}$$

and let $\{\phi_1, \cdots, \phi_n\}$ and $\{\mu_1, \cdots, \mu_n\}$ the n the basis functions for the space V_h and M_h respectively, we construct the functions μ_i using the following biorthogonality property between the space V_h and M_h:

$$\int_\Omega \mu_i \phi_j \, dx = c_j \delta_{ij} \,, \ \ c_j \neq 0 \,, \ \ 1 \leq i, j \leq n \,, \tag{18}$$

where δ_{ij} is Kronecker symbol, and c_j is a scaling factor which can be chosen to be proportion al to the area of support of ϕ_j. The local basis function of K_h and M_h for the reference square element (see figure 1) $\hat{T} := \{(\xi, \eta) : -1 \leq \xi \leq 1 \,, -1 \leq \eta \leq 1\}$ are:

$$\begin{aligned} \phi_1 &= \frac{1}{4}(1-\xi)(1-\eta) \,, \quad \phi_2 = \frac{1}{4}(1+\xi)(1-\eta) \,, \\ \phi_3 &= \frac{1}{4}(1+\xi)(1+\eta) \,, \quad \phi_4 = \frac{1}{4}(1-\xi)(1+\eta) \,. \end{aligned} \tag{19}$$

and

$$\begin{aligned} \mu_1 &= 1 - 3\xi - 3\eta + 9\xi\eta \,, \quad \mu_2 = 1 + 3\xi - 3\eta - 9\xi\eta \,, \\ \mu_3 &= 1 + 3\xi + 3\eta + 9\xi\eta \,, \quad \mu_4 = 1 - 3\xi + 3\eta + 9\xi\eta \,. \end{aligned} \tag{20}$$

It is important to observe that the global basis functions of the space M_h are not continuous.

4.1. Bubble functions

In this section we detail the different choosing of the bubble functions. Addition of the bubble functions is essential to create a stable space. we have four types of bubbles. In the first two cases we use a modification of the standard bubble function ,that is for the reference element:

$$b_T(\xi, \eta) = (1 - \xi^2)(1 - \eta^2) \,, \tag{21}$$

while in the next two, we add to the standard bubble function another one.

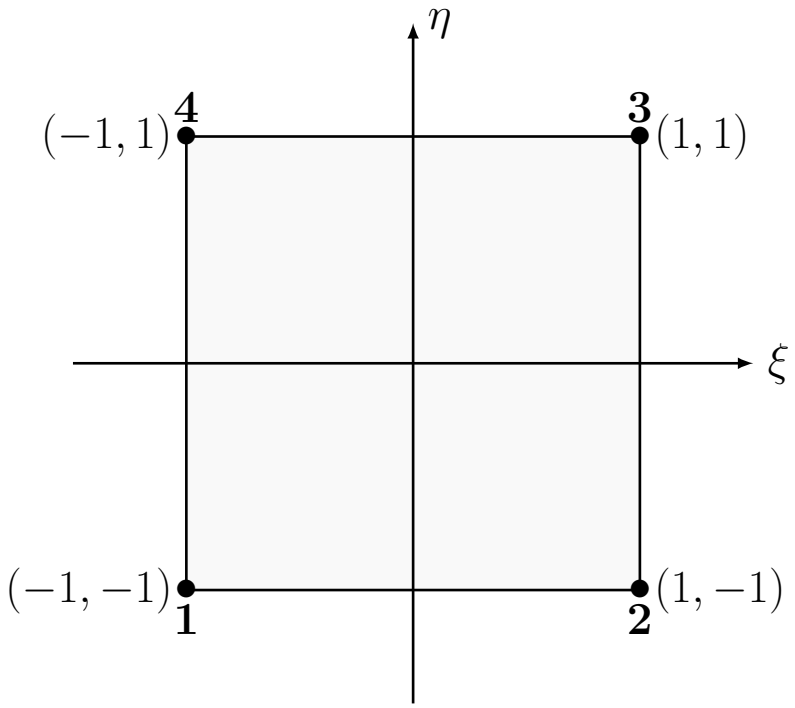

Figure 1: Reference Element

4.1.1. One Bubble function (type 1)

As a first choice of bubble function we use:

$$\hat{b}_T(\xi,\eta) = c_T \cdot \phi_T(\xi,\eta) \cdot b_T(\xi,\eta)\,, \tag{22}$$

where c_T is a coefficient in order to obtain $\hat{b}_T(\xi_g,\eta_g) = 1$ (where $\boldsymbol{g}$ is the centroid of the elements), ϕ_K is the standard bilinear basis function corresponding to the lower-left corner of the square T. In the case of reference square element we obtain:

$$\hat{b}_T(\xi,\eta) = (1-\xi)(1-\eta)(1-\xi^2)(1-\eta^2)\,. \tag{23}$$

4.1.2. One Bubble function (type 2)

The second choice of bubble function we take:

$$\hat{b}_T(\xi,\eta) = c_T \cdot (a + b\xi + c\eta) \cdot b_T(\xi,\eta)\,, \tag{24}$$

where $a, b, c \in \mathrm{R}$ and $a, b, c \neq 0$. For simplicity we set $a = b = c = 1$ and we obtain for the reference square:

$$\hat{b}_T(\xi, \eta) = (1 + \xi + \eta)(1 - \xi^2)(1 - \eta^2) \,. \tag{25}$$

4.1.3. Two Bubble functions

Using two bubble functions, where the first is the standard bubble function and the second bubble is a modification of the standard bubble:

$$\begin{aligned} \hat{b}_{T1}(\xi, \eta) &= b_T \,, \\ \hat{b}_{T2}(\xi, \eta) &= c_T \cdot (a\xi + b\eta) \cdot b_T \,, \end{aligned} \tag{26}$$

where $a, b \in \mathrm{R}$ and $a^2 + b^2 \neq 0$. For the sake of simplicity we adopt $a = b = 1$. One obtains:

$$\begin{aligned} \hat{b}_{T1}(\xi, \eta) &= (1 - \xi^2)(1 - \eta^2) \,, \\ \hat{b}_{T2}(\xi, \eta) &= (\xi + \eta)(1 - \xi^2)(1 - \eta^2) \,. \end{aligned} \tag{27}$$

4.1.4. Two Bubble functions, which one mixed

As a finally choice of bubbles we use a standard bubble function plus one mixed bubble function for the two components of displacement.

$$\begin{aligned} \hat{b}_{T1}(\xi, \eta) &= b_T \,, \\ \hat{b}_{T2,\xi}(\xi, \eta) &= (\nabla \phi_1)_\xi \cdot b_T \,, \\ \hat{b}_{T2,\eta}(\xi, \eta) &= (\nabla \phi_1)_\eta \cdot b_T \,, \end{aligned} \tag{28}$$

where $(\nabla \phi_1)_i$ is i-th component of the gradient of the first shape function ϕ. In this way we have as shape function for the displacement using the mixed bubble function the vector $\left[\hat{b}_{T2,x}(x, y), \hat{b}_{T2,y}(x, y)\right]$.

5. Numerical example

In this section we report some examples using the presented formulation to proven the good behaviour.

5.1. Square problem

First example is a unit square domain with homogeneous Dirichlet boundary conditions. This benchmark problem is analyzed in S.C. Brenner (1993). The Lamé constant are fix to $\nu = 0.49995$ and $\mu = 1$. We impose the body forces in using the following expressions: f

$$\begin{aligned} f_1 &= \beta \left(\pi^2 \left(4 \sin\left(\pi y\right) \left(-1 + 2\cos\left(2\pi x\right)\right) - \cos\left(\pi\left(x+y\right)\right) \right.\right. \\ &\quad \left.\left. + A \sin\left(\pi x\right) \sin\left(\pi y\right)\right)\right) , \\ f_2 &= \beta \left(\pi^2 \left(4 \sin\left(2\pi x\right) \left(1 - 2\cos\left(2\pi y\right)\right) - \cos\left(\pi\left(x+y\right)\right) \right.\right. \\ &\quad \left.\left. + A \sin\left(\pi x\right) \sin\left(\pi y\right)\right)\right) , \end{aligned} \tag{29}$$

where

$$A = \frac{2}{1+\lambda} \text{ and } \beta = \frac{1}{25} . \tag{30}$$

By imposition of the previously body forces the exact solution is:

$$\begin{aligned} u_1 &= \beta \left(\sin\left(2\pi y\right) \left(-1 + \cos\left(2\pi x\right)\right) + B\right) , \\ u_2 &= \beta \left(\sin\left(2\pi x\right) \left(1 - \cos\left(2\pi y\right)\right) + B\right) , \end{aligned} \tag{31}$$

where

$$B = 0.5 A \sin\left(\pi x\right) \sin\left(\pi y\right) . \tag{32}$$

The problem is study using two type of mesh: first of all using a square mesh and before using a trapezoidal mesh. The two types of mesh are shown in figures 2(a) and 2(b). Figures 3(a), 3(b), 4(a) and 4(b) shown the error in norm L^2 in the case of regular mesh for the different types of bubble functions used and types of coefficient α. All types of element converge in a good way. In Figures 5(a), 5(b), 6(a) and 6(b) we report the previously results in the case of trapezoidal meshes.

5.2. Cantilever beam problem

Now we consider the beam with length $L = 10$ and height $l = 2$ as we shown in figure 11. The Young modulus is set equal to $E = 1500$ and the Poisson $\nu = 0.4999$ and subjected to a distributed load as in figure 11 with $f = 300$. The exact solution is:

$$\begin{aligned} u(x,y) &= \frac{2f}{El}(1-\nu^2)x\left(\frac{l}{2} - y\right) , \\ v(x,y) &= \frac{f}{El}\left[x^2 + \frac{\nu}{1-\nu}\left(y^2 - ly\right)\right] . \end{aligned} \tag{33}$$

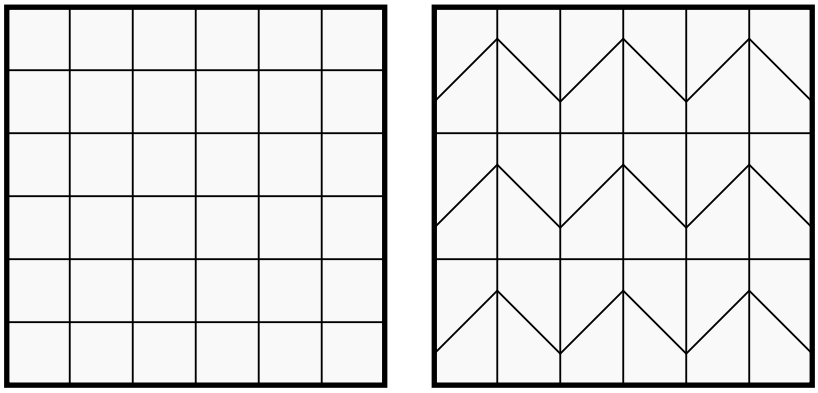

(a) Regular mesh (b) Trapezoidal mesh

Figure 2: Square Problem

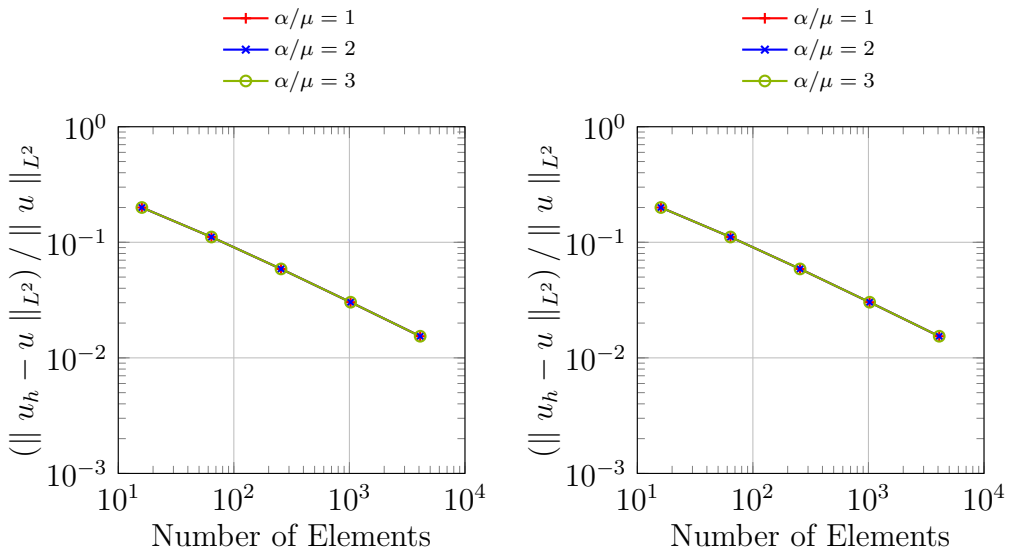

(a) type 1 (b) type 2

Figure 3: The relative error vs. the number of elements measured relative to the L^2 norm (Case one bubble function and regular mesh)

We use to model the beam two types of mesh: regular anf trapezoidal as in the previously example (see figures 2(a) and 2(b)). we shown in figures

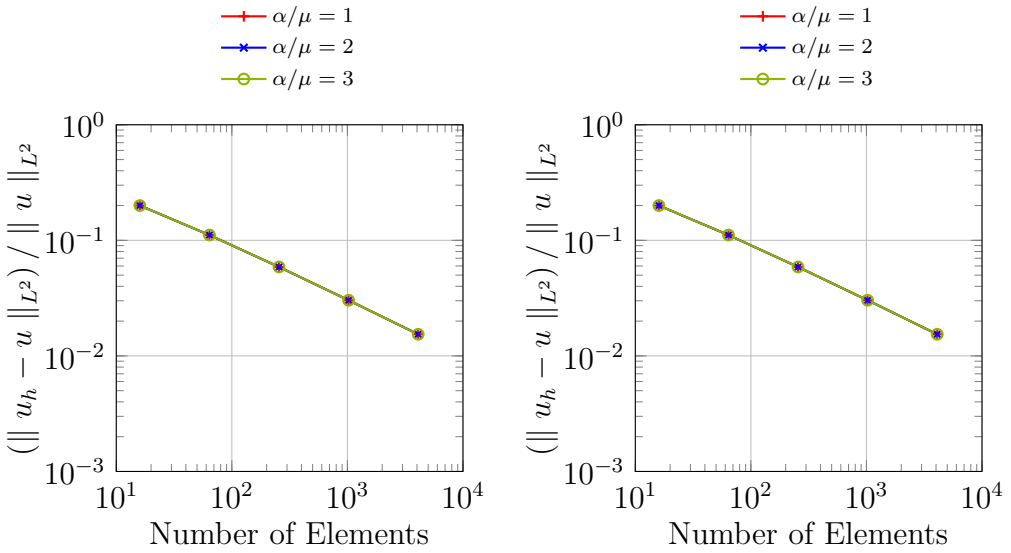

(a) Case two bubble function

(b) Case two bubble function of which one mixed

Figure 4: The relative error versus the number of elements measured relative to the L^2 norm (regular mesh)

15(a), 15(b), 16(a) and 16(b) the L^2-norm error for different types of bubble functions used in the case of $\alpha/mu := 1, 2, 3$, while in figures 15(a), 15(b), 16(a) and 16(b) the same plots using trapezoidal meshes. In the all cases the elements distorted have a good behaviour respect to the regular mesh.

5.3. Cook's membrane

The final example is the Cook's membrane. That is a typical benchmark and consist of a beam with vertex: $(0, 0)$, $(48, 44)$, $(48, 60)$ and $(0, 44)$. The left vertical edge is clamped and the right vertical edge subjected to the vertical distributed forces with resultant $F = 100$ as it shown in figure 17. The material properties are taken to be $E = 250$ and $\nu = 0.4999$, so that a nearly incompressible response is obtained. We report in figures 18(a), 18(b), 18(c) and 18(d) the vertical displacement of the point A versus the number of element per side for different choosing of the parameter $\alpha = \{1, \mu, 2\mu, 3\mu\}$. All elements return different behaviour using different coefficients α. In the case of $\alpha = 1$, figure 18(a), the obtained results completely not converge to the reference solution.

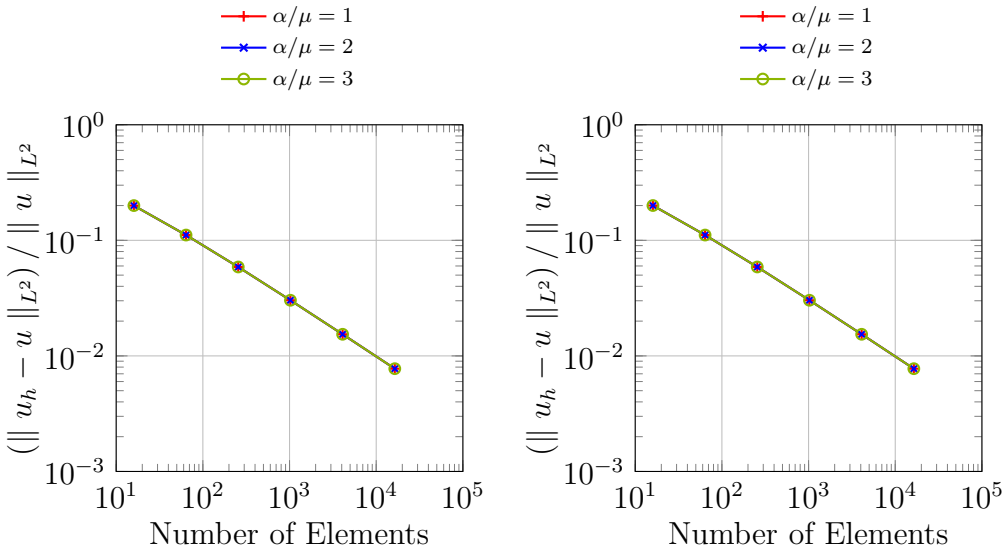

(a) type 1 (b) type 2

Figure 5: The relative error vs. the number of elements measured relative to the L^2 norm (Case one bubble function and Trapezoidal mesh)

6. Conclusions

We present a new family of quadrilaterals mixed finite elements based on a modified Hu-Washizu formulation. We test the different types of enrichment and confirm the robustness of all elements created. Uniform convergence are archived in the incompressible regime. We study the robustness of the elements in the case of trapezoidal meshes. The extension to the 3D case using hexahedra is straightforward.

W.Bai. "The quadrilateral 'Mini' finite element for Stokes problem", *Comput. Methods Appl. Mech. Engrg.*, 143: 41-47, 1997.

D.Boffi. "On the finite element method on quadrilateral meshes", *Appl. Num. Mathematics*, 56: 1271-1282, 2006.

B.P.Lamichhane. "A quadrilateral 'mini' finite element for the Stokes problem using a single bubble function", *Appl. Num. Math.*, 56: 1271-1282, 2015.

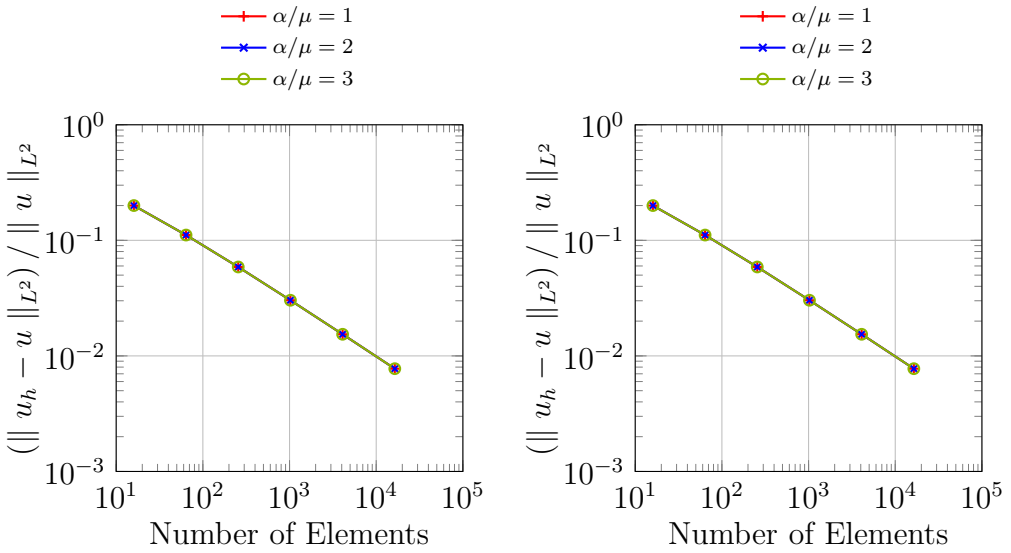

(a) Case two bubble function

(b) Case two bubble function of which one mixed

Figure 6: The relative error vs. the number of elements measured relative to the L^2 norm (Case one bubble function and Trapezoidal mesh)

J.K.Djoko, B.D.Reddy. "An extended Hu-Washizu formulation for elasticity", *Comput. Methods Appl. Mech. Engrg.*, 195: 6330-6346, 2006.

B.P.Lamichhane, A.T.McBride, B.D.Reddy. "A finite element method for three-field formulation of linear elasticity based on biorthogonal systems", *Comput. Methods Appl. Mech. Engrg.*, 258: 109-117, 2013.

B.P.Lamichhane, B.D.Reddy, B.I.Wohlmuth. "Convergence in the incompressible limit of finite element approximation based on Hu-Washizu formulation", *Numer. Math.*, 104: 151-175, 2006.

D.Boffi, C.Lovadina. "Analisys of new augmented Lagrangian formulation for mixed finite element schemes", *Numer. Math.*, 75: 405-419, 1997.

B.P.Lamichhane. "From the Hu-Washizu formulation to the average nodal strain formulation", *Comput. Methods Appl. Mech. Engrg.*, 198: 3957-3961, 2009.

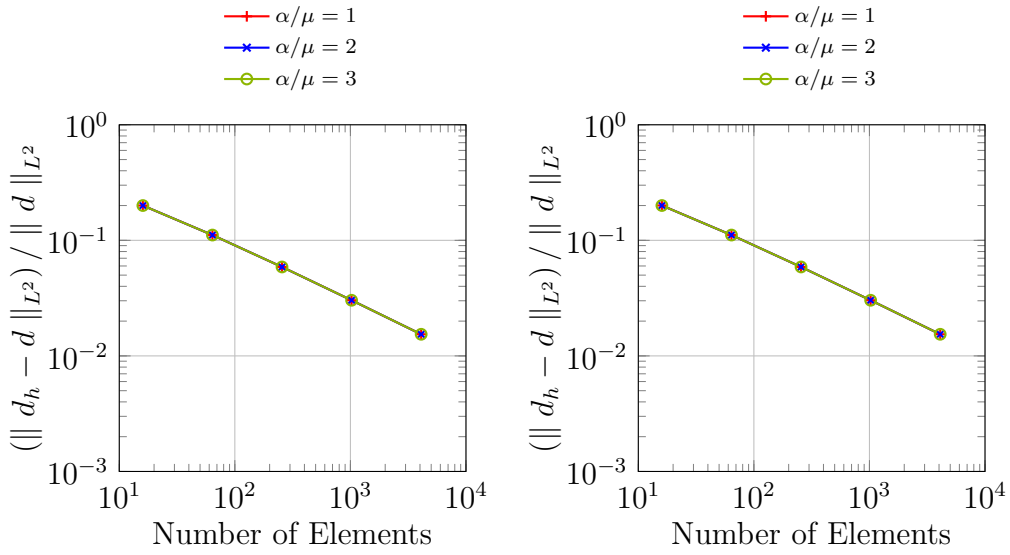

(a) Case regular mesh

(b) Case trapezoidal mesh

Figure 7: The relative error of strain $\boldsymbol{d}_{xx}$ vs. the number of elements (Case of two bubble functions)

D.N.Arnold, R.Winther. "Mixed finite elements for elasticity", *Numer. Math.*, 92: 401-419, 2002.

D.Boffi, F.Brezzi, M.Fortin. "Mixed Finite Element Methods and Applications", *Springer Series in Computational Mathematics*, Vol.44, 2013.

D.N.Arnold, G.Awanou. "Rectangular mixed finite elements for elasticity", *Models Methods Appl. Sci.*, 15: 1417-1429, 2005.

H.Hu. "On some variational principles in the theory of elasticity and the theory of plasticity", *Sci. Sin.*, 4: 33-54, 1955.

K.Washizu. "Variational Methods in Elasticity and Plasticity, third ed.", *Pergamon Press*, 1982.

B.M. Fraeijs de Veubeke. "Diffusion des inconnues hyperstatiques dans les voilures á longeron couplés", *Bull. Serv. Technique de l'Aeronautique Impremérie Marcel Hayez*, Bruxelles, 1951.

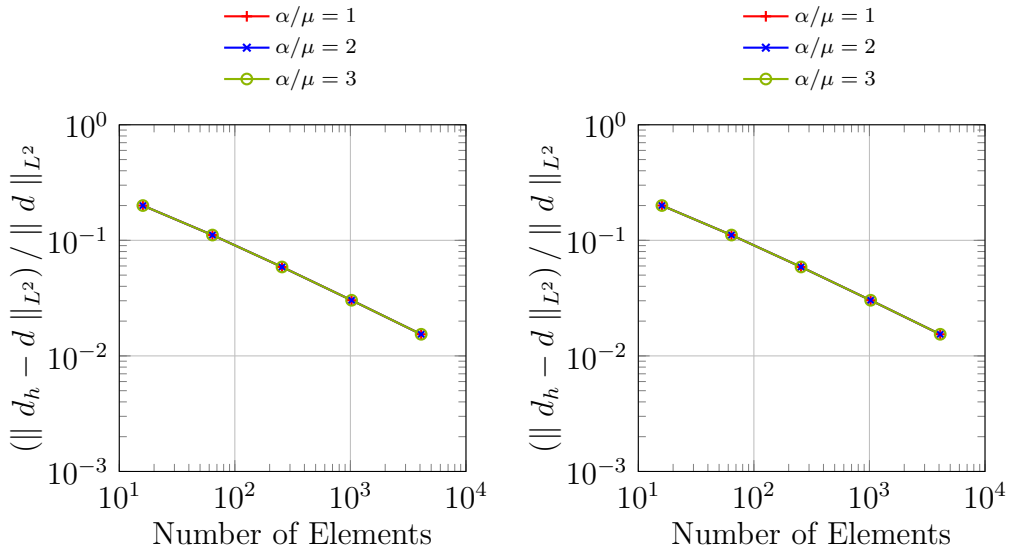

(a) Case regular mesh

(b) Case trapezoidal mesh

Figure 8: The relative error of strain $\boldsymbol{d}_{xx}$ vs. the number of elements (Case of two bubble functions, which one mixed)

E.P. Kasper, R.L. Taylor. "A mixed-enhanced strain method Part I: geometrically linear problems", *Comput. Struct.*, 75: 237-250, 2000.

E.P. Kasper, R.L. Taylor. "A mixed-enhanced strain method Part II: geometrically nonlinear problems", *Comput. Struct.*, 75: 251-260, 2000.

S.C. Brenner. "A nonconforming mixed multigrid method for the pure displacement problem in planar linear elasticity", *SIAM J. Numer. Anal.*, 30: 116–135, 1993.

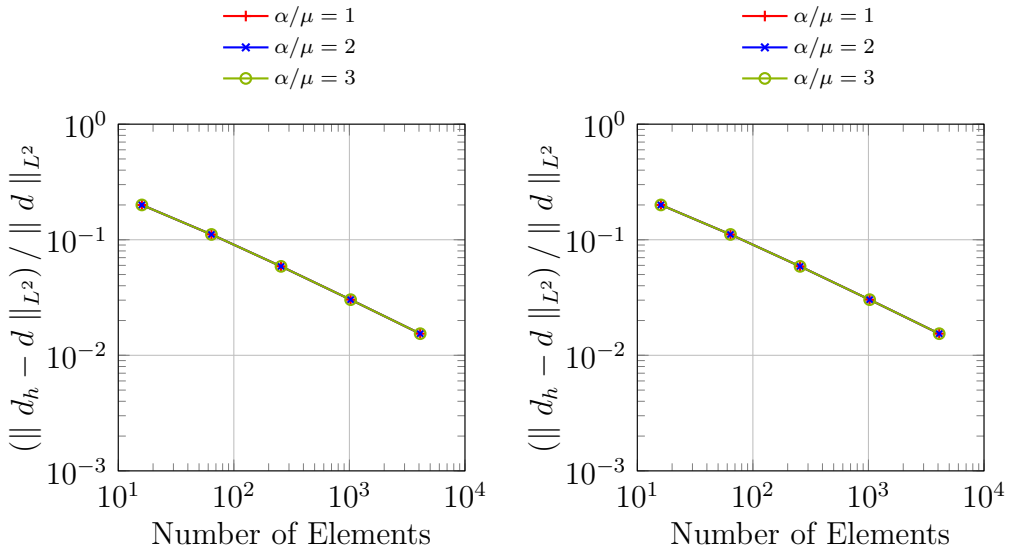

(a) Case regular mesh

(b) Case trapezoidal mesh

Figure 9: The relative error of strain $\boldsymbol{d}_{xx}$ vs. the number of elements (Case of one bubble function type 1)

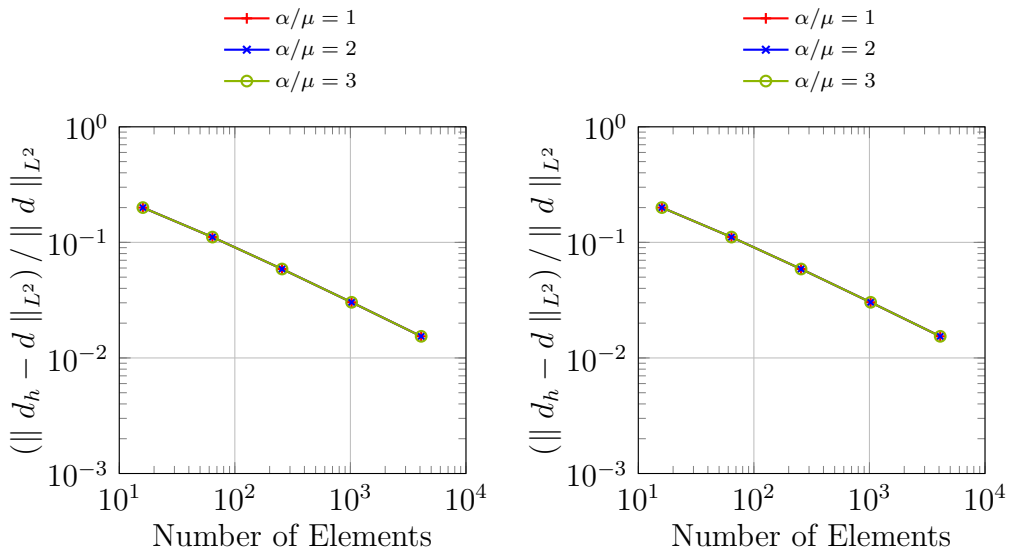

(a) Case regular mesh

(b) Case trapezoidal mesh

Figure 10: The relative error of strain $\boldsymbol{d}_{xx}$ vs. the number of elements (Case of one bubble function type 2)

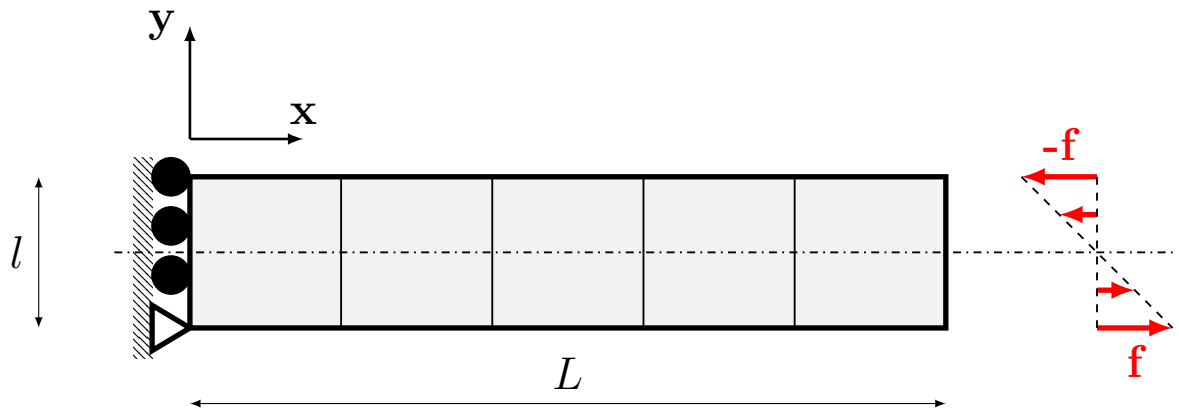

Figure 11: Beam cantilever geometry

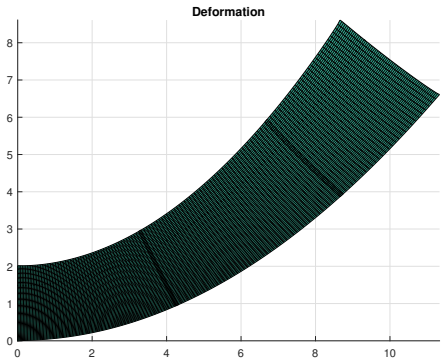

(a) Deformation

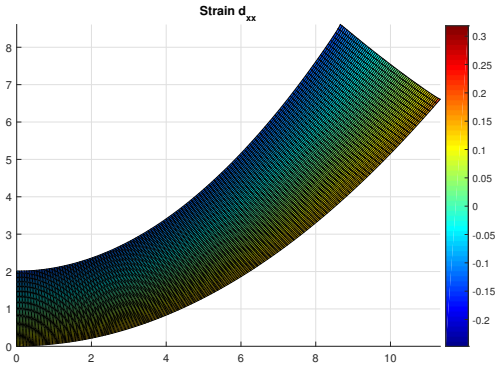

(b) Strain $\boldsymbol{b}_{xx}$

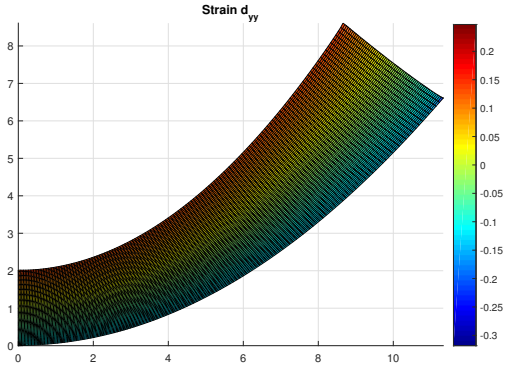

(c) Strain $\boldsymbol{b}_{yy}$

Figure 12: Beam cantilever solution using 8192 elements of two bubble functions and $\alpha/\mu = 3$

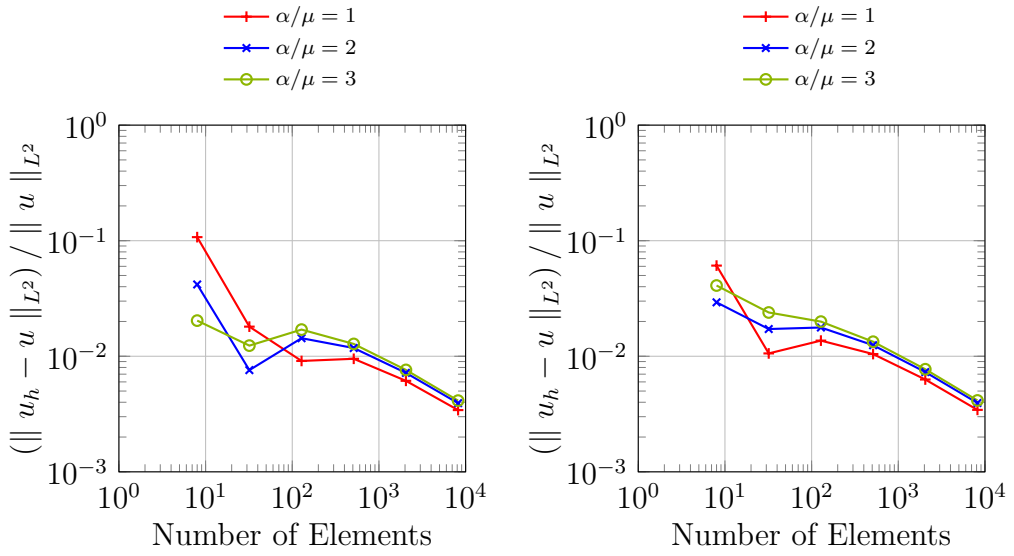

(a) Type 1 (b) Type 2

Figure 13: Beam Cantilever: the relative error vs. the number of elements measured relative to the L^2 norm (regular mesh)

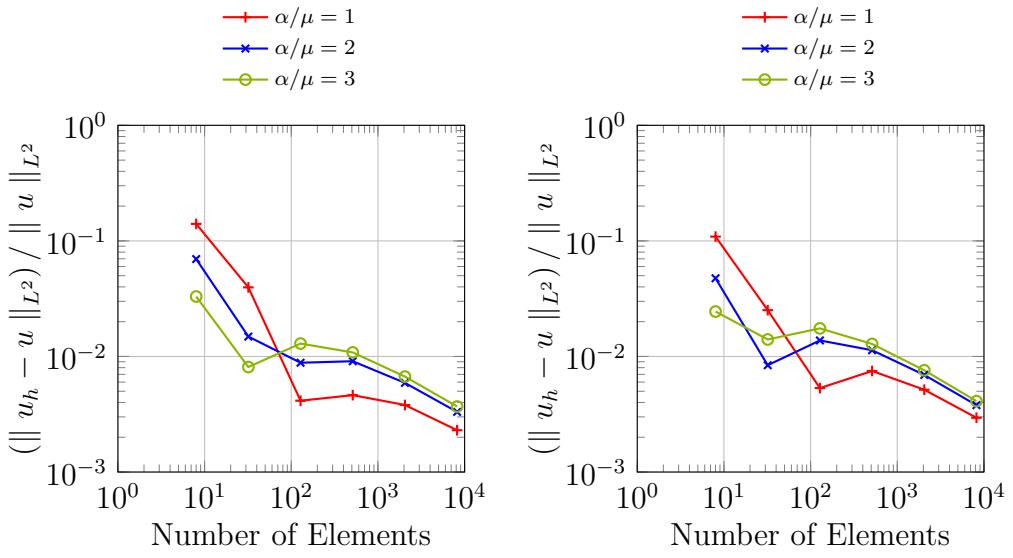

(a) Case two bubble function

(b) Case two bubble function of which one mixed

Figure 14: Beam Cantilever: the relative error vs. the number of elements measured relative to the L^2 norm (regular mesh)

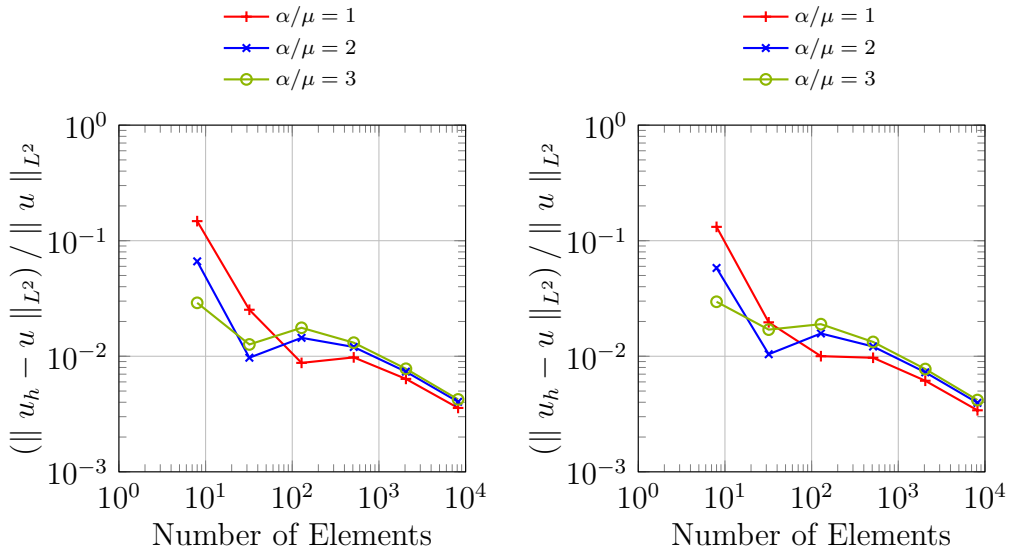

(a) Type 1

(b) Type 2

Figure 15: Beam Cantilever: the relative error vs. the number of elements measured relative to the L^2 norm (trapezoidal mesh)

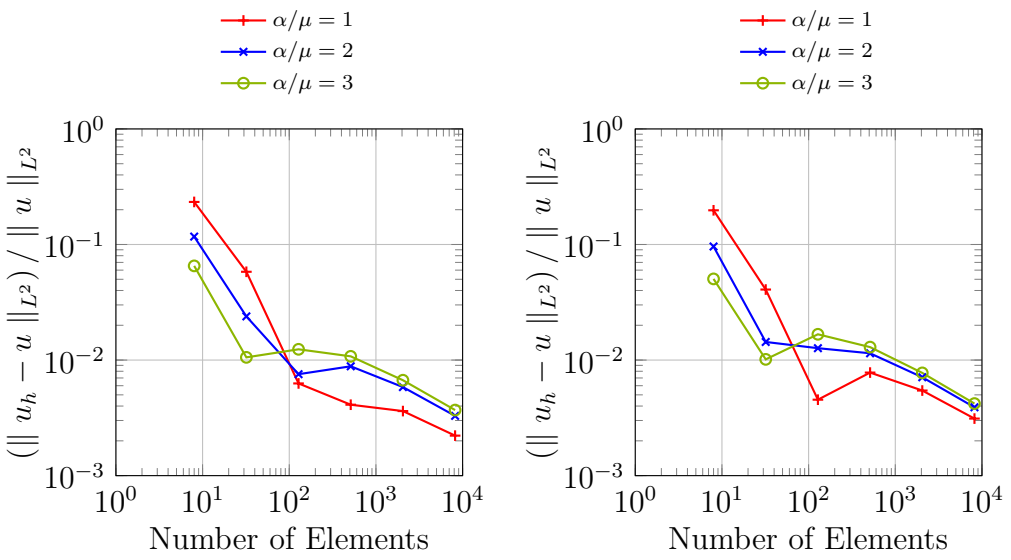

(a) Case two bubble function

(b) Case two bubble function of which one mixed

Figure 16: Beam Cantilever: the relative error vs. the number of elements measured relative to the L^2 norm (trapezoidal mesh)

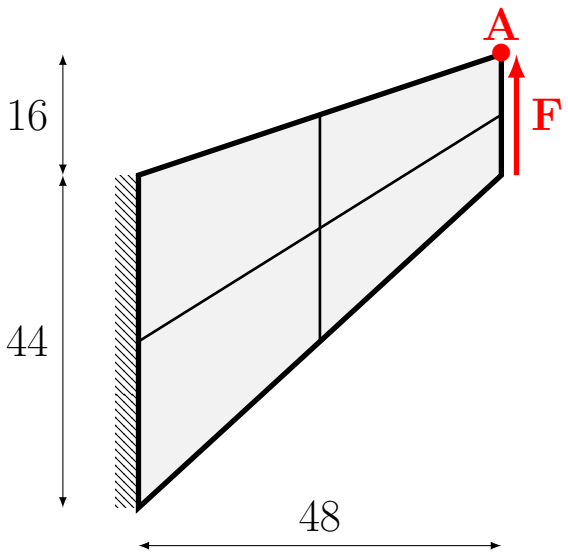

Figure 17: Cook's Membrane geometry

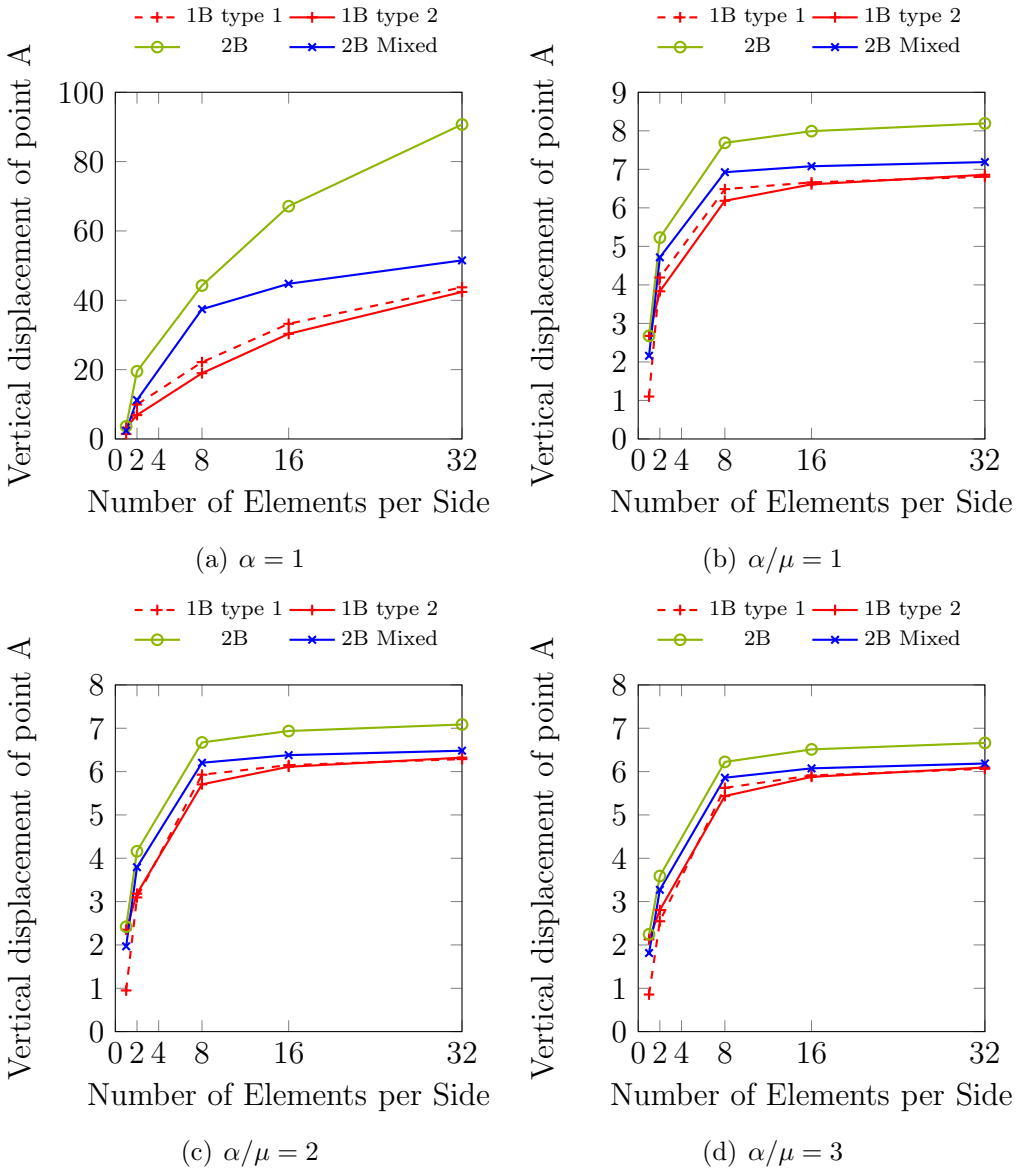

(a) $\alpha = 1$

(b) $\alpha/\mu = 1$

(c) $\alpha/\mu = 2$

(d) $\alpha/\mu = 3$

Figure 18: Vertical Displacement of point A vs. the number of elements per side